INFLUENCE OF THE GEOMETRIC AND MECHANICAL PARAMETERS ON THE TEMPERATURE EVOLUTION WITHIN THE TUBES OF A RECEIVER FROM A SOLAR POWER TOWER

Messaoud HAZMOUNE[1], Benaoumeur AOUR[2], Xavier CHESNEAU[3], Gheorghe LAZAROIU[4], Mohamed Mandji HADJIAT[5], Mohamed DEBBACHE[6], Dana-Alexandra CIUPAGEANU[7]

The receiver of a solar power tower raises many issues concerning efficiency and system safety. Hence, the analysis of the various parameters affecting the performances of the solar receiver is required. This paper aims to investigate the variation of the system's performance as a response to several modifications, such as fluid velocity variation, receiver's piping thickness modification, and change of the material. The solar tower receiver has the front half of piping heated and the behind piping surface at ambient temperature, the geometry consisting of two parts (fluid and solid) that interact. Simulations are performed with ANSYS CFX. A uniform mesh is generated by the ICEM. Thermal, mechanical and dynamic analyses of this solar receiver have been carried out. Simulation data obtained with ANSYS Fluent were compared with the experimental ones. The increase of the inlet velocity determines a decrease in the outlet temperature; the dependence between the thickness and the outlet temperature is a proportional one, as they are submitted to the conduction effect. Regarding the material analysis, the researches have shown that Alloy 625 is the most effective, because of its mechanical and thermal proprieties.

Keywords - Solar power tower, solar receiver, Ansys CFX, heat transfer.

[1] PhD Student, Laboratoire de Biomécanique Appliquée et Biomatériaux, Département de Génie Mécanique, Ecole Nationale Polytechnique d'Oran BP 1523 El Mnaour, Oran 31000, Algérie
[1] Researcher, Centre de Développement des Energies Renouvelables BP. 62 Route de l'Observatoire Bouzareah 16340 Alger, Algérie haz_mess@yahoo.fr
[2] Professor, Laboratoire de Biomécanique Appliquée et Biomatériaux, Département de Génie Mécanique, Ecole Nationale Polytechnique d'Oran BP 1523 El Mnaour, Oran 31000, Algérie ben_aour@yahoo.fr
[3] Senior Lecturer, Laboratoire de Mathématiques et Physique, Université de Perpignan Via Domitia - Bât.B - 2e étage 52 avenue Paul Alduy - 66860 PERPIGNAN Cedex France. chesneau@univ-perp.fr
[4] Professor, University POLITEHNICA of Bucharest, Splaiul Independentei 313, Sector 6, Bucharest, Romania RO-060042 glazaroiu@yahoo.com
[5] Researcher, Centre de Développement des Energies Renouvelables BP. 62 Route de l'Observatoire Bouzareah 1 6340 Alger, Algérie mhadjiat@gmail.com
[6] Researcher, Centre de Développement des Energies Renouvelables BP. 62 Route de l'Observatoire Bouzareah 16340 Alger, Algérie md.debbache@gmail.com
[7] PhD Student, University POLITEHNICA of Bucharest, Splaiul Independentei 313, Sector 6, Bucharest, Romania RO-060042, dana_ciupageanu@yahoo.com.

1. Introduction

Worldwide, the energy sector depends on fossil fuels for balancing the demand in medium and long-term horizon. The intensive use of these natural resources are responsible for climate changes, as their exploitation generates harmful emissions [1]. Renewable energy sources are regarded as the alternative to fossil fuels. In the context of electricity generation, solar energy is an inexhaustible source of clean energy [2], [3]. Moreover, it is remarked that lately solar concentrating technologies recorded a boost, not only technically but also commercially. [4]. The basis of these technologies relies on the collectors that concentrate the solar radiation towards the heat transfer fluid with high temperature. Further, this fluid is used to generate the steam that will enter an electricity generation section (based, for instance, on Rankin cycle) [5]. The performance analysis of a solar receiver using molten salt represents one of the main topics to be addressed in the field of heat transfer in solar power plants [6]. The receivers play an important role in collecting solar radiation, converting and transmitting the heat employing a heat transfer fluid to the storage system or the power block. In some receivers, the flow is perpendicular to the direction of incidence of solar radiation [7].
In solar power plants with the central receiver, the sun radiation is reflected by the heliostats and concentrated on the receiver as shown in Figure.1.The energy flux incident on the receiver is transferred to the fluid HTF (molten salts, water steam, liquid sodium or air).

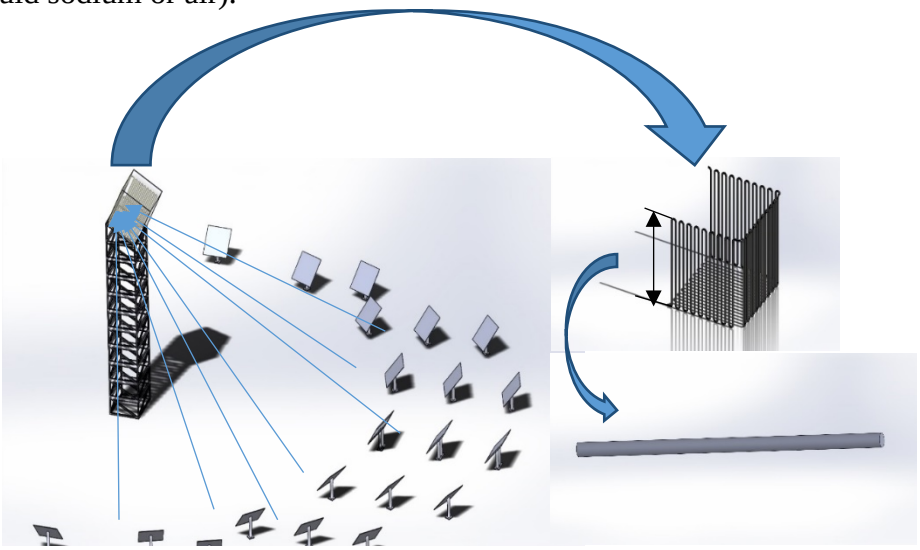

Fig. 1. Tubular receiver of a central solar power tower.

Aiming to control the temperature changes caused by the heat variation determined by the absorbed radiation at solar tower receiver. This paper presents a study on the thermal behavior of solar tower receiver piping. The effects of the flow velocity in

turbulent flow, the piping thickness and of the material employed are taken into account.

2. Literature review

Recently, several of researches have been done on solar concentration technology especially the receiver part. Nicholas Boerema et al. [8] studied the behavior of different designs to determine the surface temperature of tubular panels. Oliver Garbrecht et al. [9] introduced a new concept for the receiver of a solar power tower, in which molten salt is used as a coolant and the geometry comprises multiple hexagonal pyramids arranged with their vertices pointing to the heliostats. This new receiver has a thermal efficiency of 91.2% and allows reducing the losses through reflection of the incident radiation by 1.3%. Javier Samanes and Javier Garcia Barberena [10] presented a detailed work on cavity solar receivers used in solar power towers, The study aimed to investigate the major phenomena affecting the performance of a cavity receiver by considering all types of heat transfer (radiation, convection and conduction). The receiver considered was able to predict the transient performance of a cavity receiver over long periods for different parameters. The work was performed by simulation, using the molten salt as a heat transfer fluid, the results showing the fiability of the model and the convenience of implementation.

In 2011, M.J. Montes et al. [11] published a paper regarding a new thermo-fluid dynamic design of a solar central receiver, discussing the optimized heat transfer in the absorber surface. Also, a new design for the absorber surface active central receptors was presented. They demonstrated that increasing the coefficient of convection of the fluid enables enlarging its velocity.

M.R. Rodríguez-Sánchez et al. [12] analyzed the thermal behavior of a solar power tower receiver with molten salt. The variations of the wall temperature are included to minimize the volume of computing. The results showed that changes in wall temperature has a significant effect on the radiation losses at the receiver. In addition, the number of panels and the piping diameter have a considerable effect on the thermal, mechanical and hydrodynamic parameters of the receiver, given that the pressure dropps are determined by the increases of panels number having small diameter.

María Reyes Rodríguez-Sà et al. [13]developed two numerical models for a solar power tower receiver. The models intended to define the axial and circumferential variations of the wall temperature and the heat flux absorbed by the receiver piping. Similar results for both models have been presented, the change in the temperature of the molten salt due to the heat flux absorbed by the receiver piping being negligible.

Yu Qiu et al. [7] built a prototype to study the heat transfer process of molten salt within the receivers piping (RB-STHX).The results obtained provided reliable

experimental data and reliable correlations. Furthermore, it gave a useful guidance for building RB-STHX based on molten salts as heat transfer fluid in CSP systems.
Julian D. Osorio et al. [14] established a thermodynamic model for each component of the solar tower receiver. This work aimed to study the operation of a concentrated CSP in different seasonal conditions and the transient behavior with supercritical CO_2.
Xiaoping Yang et al [15] presented an important study in the field of solar receivers, focusing on a 1 m long receiver tube with molten salt as heat transfer fluid; the receiver pipe was heated by a heat flux in an external wall, the other wall being adiabatic. The results proved that the heat flux of the heating surface increases simultaneously with the velocity. The Sieder - Tate formula is not reliable for heat transfer in solar receiver piping, as the gradient of the temperature between the molten salt and the piping wall is very high.
Abdelrahman El-Leathy et al. [6] designed a systematic model to develop a thermal energy storage system (TES) that operates at high temperatures. Their results demonstrate that the thermal performance of a TES bin constructed with available materials.
Jean-Francois et al. [16] published a parametric study examining the influence of variations on bed design. Compared the performance of local thermal equilibrium and local non-thermal equilibrium models in the simulation of an air-rock compact bed, operating hypothetically in a CSP with an open volumetric receiver.

3. Model description and operation

The geometrical model of single tube receivers shown in Figure.2. Specifically, the length of the tube is equal to 1 m, its inside diameter is 16 mm (fluid) and the tube thickness is 2 mm (solid). One side of the receiver is superheated by solar radiation flux and the other side is adiabatic. The heat transfer fluid used is the molten salt $NaNO_3$-$NaNO_2$ -KNO_3 having the thermodynamic properties as given in [17]. The thermal conductivity and specific heat capacity are supposed to be constant 0.571 W/m.K and 1560 J/ Kg.K respectively. Table 1 lists the thermodynamic properties of molten salt.

Table 1.

Thermodynamic properties of molten salt

Mol %	Formula Weight (g/mol)	Freezing/ Melting Point (K)	Boiling Point (K)	Density (kg/m^3)	Specific Heat Capacity (J/kg K)	Viscosity (Pa·s)	Thermal conductivity (W/m K)	Prandtl No.
7- 49 - 44 (7-40-53)	1.77- 1.98	415	1843	1790	1560	0.0013- 0.0016	0.51- 0.605	4.0

The material used is Nickel-Chrome alloy 625, which proves great mechanical strength characteristics, exceptional corrosion resistance and remarkable manufacturability. The temperatures fall within the range from cryogenic level up

to 980 ° C, solidifying the Molybdenum-Niobium solution on the Nickel-Chromium matrix of 625 Alloy giving it a good mechanical resistance.

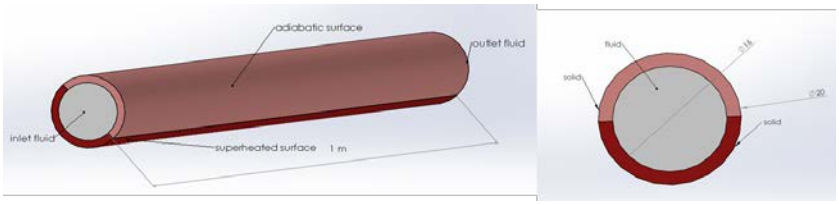

Fig. 2. Tubular receiver piping.

4. Computing equipment

Numerical simulations are carried out in ANSYS CFX Multiphysics computing software, using computing machine with 48 cores and 64 GB of memory. The results are showed in 3D in Fig. 3. The mesh configuration selection plays an important role in the accuracy of the results [18]. Several structures are considered for the mesh, as detailed in Table.2. In this context, the evaluation of its impact is tackled in next section by comparing several simulation outcomes. This paper aims to determine compromise solution between the computational burden and a satisfactory calculation precision.

Table 2

Mesh study cases

case	Fluid	Solid
1	100×40×20	100×20×10
2	200×40×20	200×20×10
3	300×50×40	300×40×20
4	300×60×40	300×50×30
5	300×80×60	300×60×40

The mesh built in simulation is presented in Fig. 3.

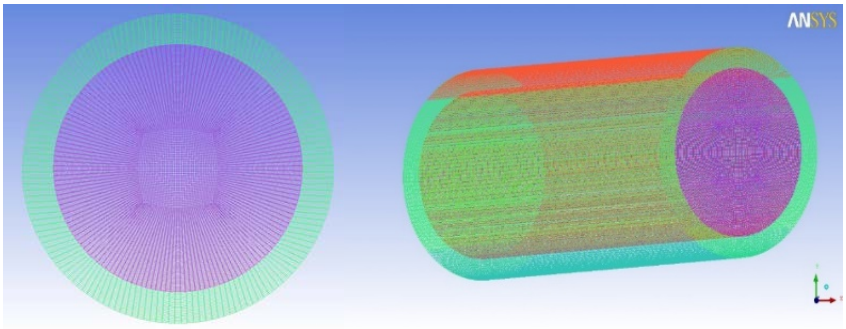

Fig. 3. Typical computational grid for numerical analysis.

5. Mathematical model

Using the conservation of mass, momentum and energy in time averaged tensor notation, the steady state equations are listed forward:

Continuity:
$$\frac{\partial \overline{u_i}}{\partial x_i} = 0 \tag{1}$$

Momentum:
$$\rho \overline{u_j} \frac{\partial \overline{u_i}}{\partial x_i} = \frac{\partial \overline{p}}{\partial x_i} + \frac{\partial}{\partial x_j}\left[\mu \frac{\partial \overline{u_i}}{\partial x_j} - \rho \overline{u_i' u_j'} \right] + \rho g_i \tag{2}$$

Energy:
$$\rho \overline{u_j} \frac{\partial \overline{T}}{\partial x_j} = \frac{1}{c_p} \frac{\partial}{\partial x_j}\left[k \frac{\partial \overline{T}}{\partial x_j} - \rho c_p \overline{T' u_j'} \right] \tag{3}$$

6. Turbulence modeling

The change of flow direction after leaving the pipe creates turbulence into the molten salt flow, significantly affecting the heat transfer process. Modeling the turbulence is very important. For this purpose, the standard $k-\varepsilon$ turbulence model has been used, with the standard wall function for the near-wall analysis. The boundary layer problem is not resolved on the mesh. A detailed description of the $k-\varepsilon$ model and its implementation in ANSYS CFX 13 is given by Launder and Spalding (1972) [19]and ANSYS (2009) [20]. The turbulent kinetic energy (K_t) and the turbulent dissipation kinetic energy (ε_t) are given as it follows:

- Turbulent kinetic energy (K_t):

$$\rho \overline{u_j} \frac{\partial \overline{k_t}}{\partial x_t} = \frac{\partial}{\partial x_j}\left[\left(\mu + \frac{\mu_t}{\sigma_{kt}} \right) \frac{\partial \overline{k_t}}{\partial x_j} \right] + P_{kt} + G_{kt} + \rho \varepsilon_t \tag{4}$$

Turbulent kinetic energy Dissipation (ε_t):

$$\rho u_j \frac{\partial \varepsilon_t}{\partial x_j} = \frac{\partial}{\partial x_j}\left[\left(\mu + \frac{\mu_t}{\sigma_{\varepsilon t}} \right) \frac{\partial \overline{\varepsilon_t}}{\partial x_j} \right] + c_{1\varepsilon_t} \frac{\varepsilon_t}{k} \left[P_{kt} + c_{3\varepsilon t} G_{kt} \right] - c_{2\varepsilon_t} \rho \frac{\varepsilon_t^2}{k_t} \tag{5}$$

The mean Nusselt number is defined:

$$Nu_m = \frac{d}{\lambda} \frac{q}{\left(T_w - T_f \right)} \tag{6}$$

The Reynolds number is given by:

$$R_e = \frac{\rho \upsilon D}{\mu} \tag{7}$$

7. Results validation

The simulation results are compared with the experimental and simulation results presented in [15], which are taken as reference. Figure 4 shows similar values (simulations conducted in this paper compared to the reference) in reference to the temperature and the Nusselt number as a function of Reynolds number. Very small differences can be noticed because the molten salt properties are not identical in simulation an in experimental conditions. It is highlighted that higher differences arise in Nu number values between refence and simulation results at lower pressures.

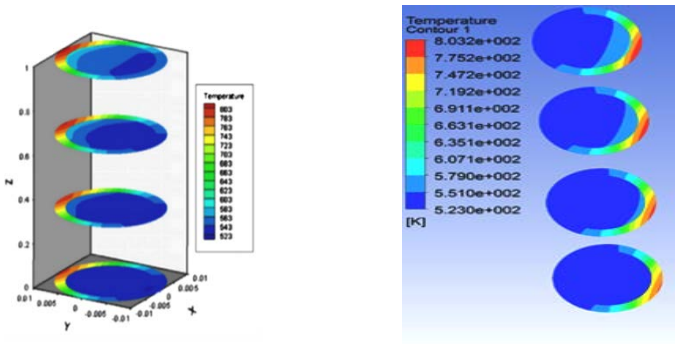

(a)

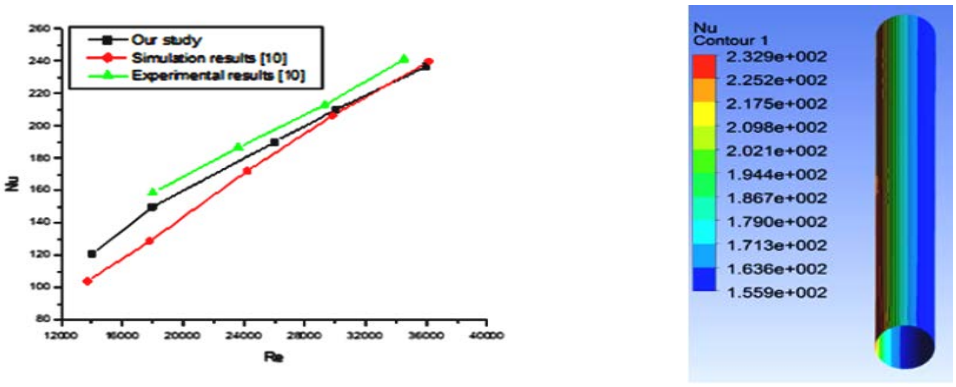

(b)

Fig. 4. Validation results, **(a)** the temperature distribution at different cross-section of tube receiver. **(b)**The comparison of the numerical and experimental Nu numbers.

7.1. Thickness influence on the temperature evolution at the exit of the receiver tube

The temperature distribution along y-axis is pictured in Figure.5 and Figure 6. The piping thickness varies between 2, 2.5 and 3 mm. The results show a considerable

difference in the outlet temperature distribution among the proposed thickness designs, as shown in Figure 4 and Figure 5.The temperature decrease between the walls is influenced by the nature of the material used, which is particularly visible for 625 alloy. The maximum temperature in the outlet section of the receiver pipe increases with the increases of thicknesses, reaching 803 K for the 2 mm thickness design, 815 K for the 2.5 mm thickness design and 839 K for the 3 mm thickness respectively. This is due to the heat transfer by conduction within the tube material. If the thickness of the wall decreases, it causes decreases of the temperature gradient between the inner and outer walls and therefore a reduction of the outer wall temperature, which is the global maximum temperature.

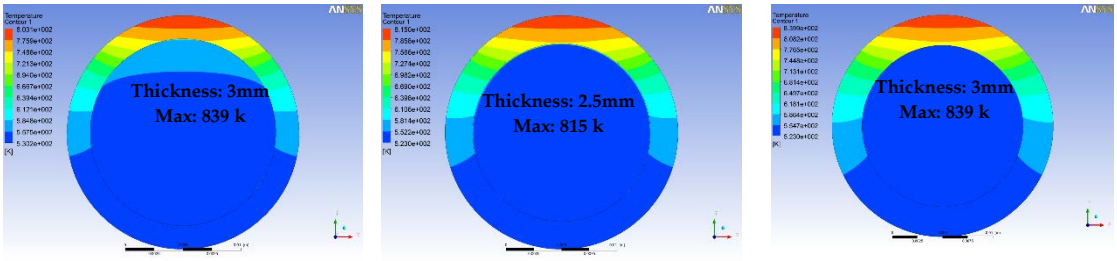

Fig. 5. Temperature distribution with different thickness of the receiver tube.

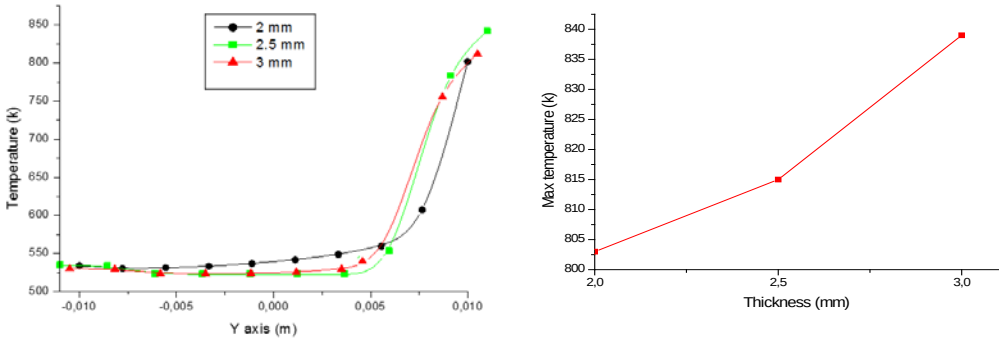

Fig. 6. Temperature evolutions according to the thickness of the receiver tube.

7.2. Velocity influence on the temperature evolution at the exit of the receiver tube

Figure 7 and Figure 8 present the different results regarding the fluid velocity variation effect in a range starting from 0.1 to 5 m/s. The thermal flow is considered equal to 0.4 Mw/m² and the inlet temperature 523 K. The temperature reaches values up to 1400 K when the velocity equals 0.1 m/s, the increasing of temperature being evident. The slow velocity of molten salt fluid particles helps it to acquire

more heat from the convective transfer between the heated receiver wall and the particles.

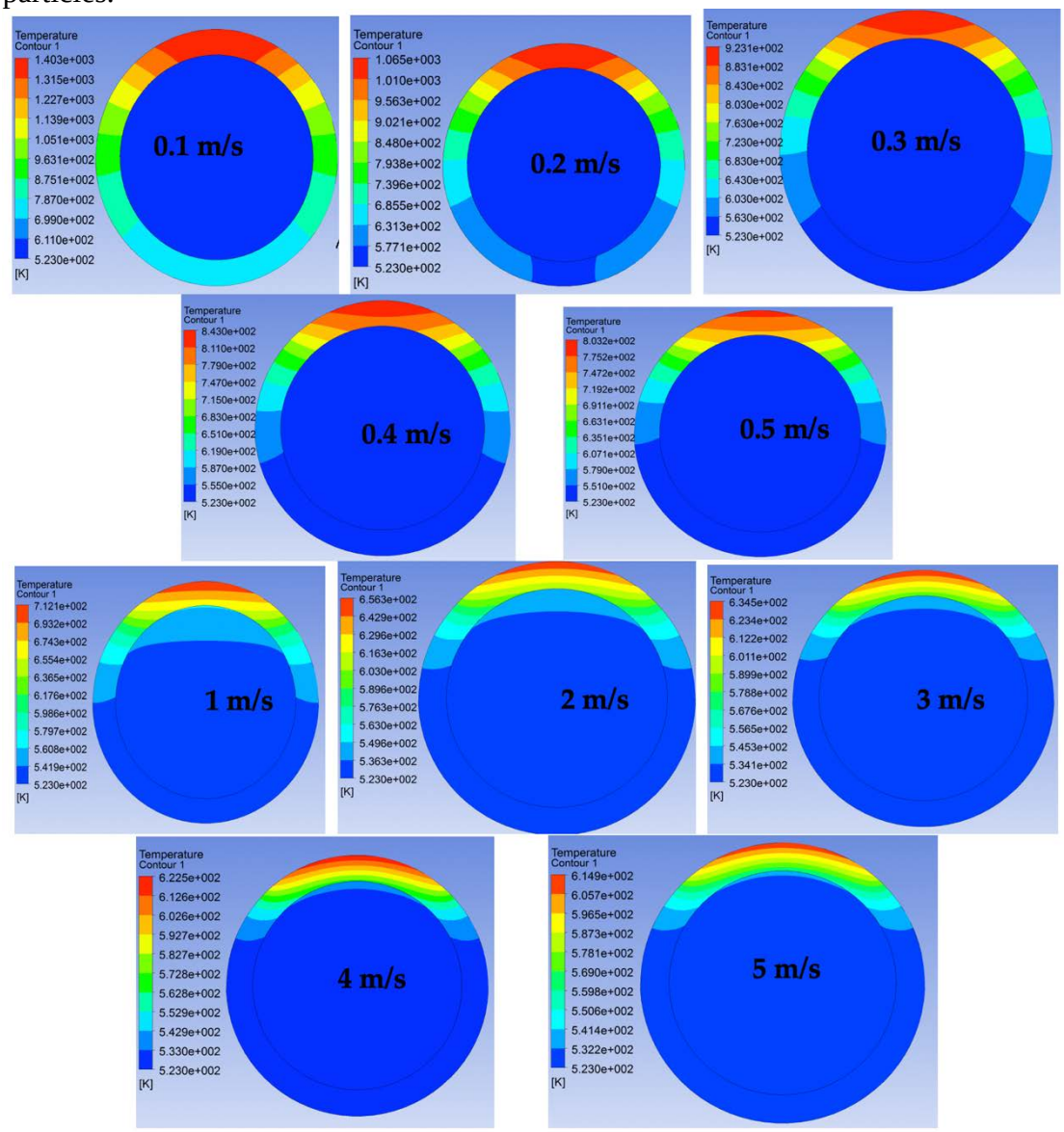

Fig. 7. Temperature distribution with different fluid velocity.

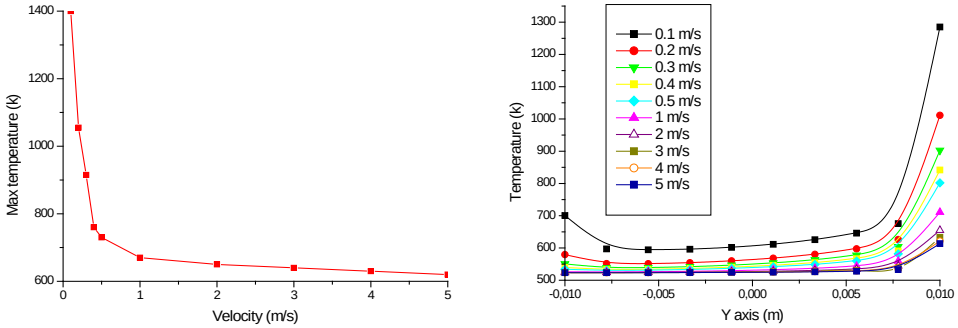

Fig. 8. Temperature evolutions according to the flow velocity.

7.3. Materials influence on the temperature profile

The thermal properties are affected by the design proposed and the materials type used, in this context, choosing the design and materials is particularly important from thermal properties aspect. To determine materials influence, five simulations test have been performed, for all five proposed materials used for manufacturing of solar receiver piping as presented in Table 3.

Figures 9 and 10 show a comparative analysis of the results obtained for several materials used in the solar receiver sector, selected based on their considerable resistance to shock, fatigue and high strength. In addition, this materials have a very good corrosion resistance. In this simulation, the inlet velocity of molten salt particles is considered equal 0.5m/s, the temperature equals 523 K and a 0.4 Mw/m² heat flux is imposed. Figure 8 and Figure 9 show that the highest temperature is obtained for alloy 625 and the lowest is registered for Copper, despite its high conductivity. According to the results, alloy 625 represents the most suitable alternative for the manufacture of solar receivers. In addition, it has a good resistance to corrosion and punctures problems, which may affect the piping thickness.

Table 3. **Thermodynamic properties of the different materials.**

Materials	Density (kg/m^3)	Thermal conductivity(W/m.K)	Specific heat capacity (J/kg ^{0}K)	Melting Point (K)
Alloy 625	8440	16.3	505	1623
AlSi12	2661	181	939	1013
Alloy 800H	7940	18.3	460	1255
Si C	3210	70	1200	1014.7
$Al_2 O_3$	3950	20	451	2369
Copper	8940	340	450	1358

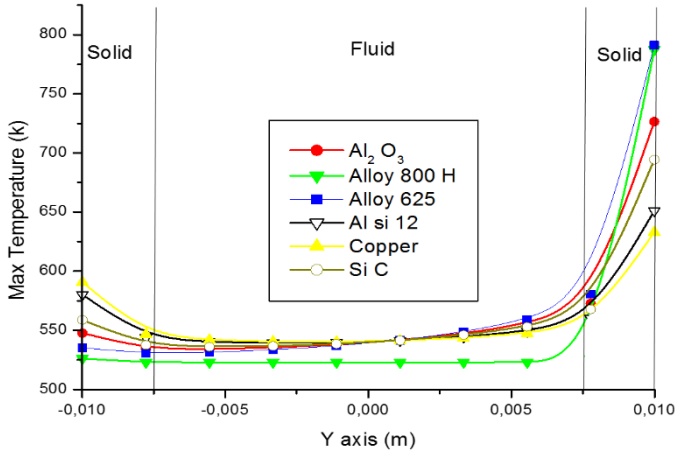

Fig. 9. Influence of the different materials on the evolution of the temperature within the receiver.

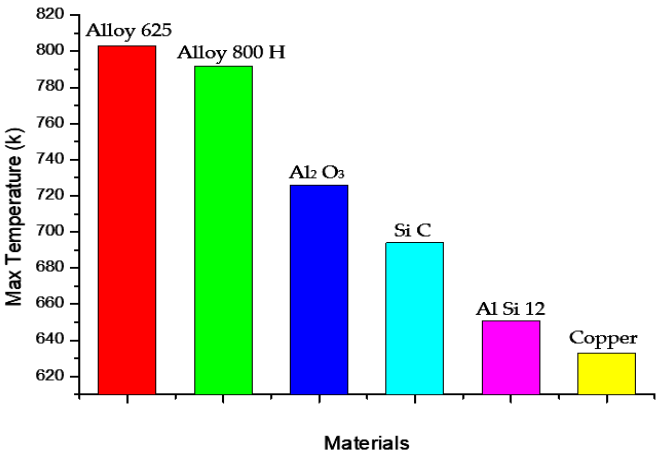

Fig. 10. Maximum temperatures within the receiver for different materials

8. Conclusion

A CFD simulation has been performed, aiming to design a tubular receiver for solar towers, using and adapting design criteria already available in the literature. This research focused on important parameters, which directly influence the temperature profile and the efficiency of the receiver, such us: the inlet velocity, tubular piping thickness and material. For this purpose, the inlet velocity varied from 0.1 m/s to 0.5 m/s. The tubular thickness took 2, 2.5 and 3 mm values and considered were alloy 625, alloy 800 H, Aluminum oxide (Al_2O_3), AlSi 12 alloy, Silicon carbide (SiC) and Copper were taken into account with respect to the material, being commonly used in solar receiver manufacturing. They have high resistance to shock and fatigue and high mechanical strength and corrosion resistance. The tubular

receiver has a diameter of 16mm, the fluid used is molten salt ($NaNO_3$-$NaNO_2$-KNO_3) and the heat flux equals 0.4 mW/m². According to the simulation results, it is highlighted that the temperature decreases as the input velocity of the receiver increases. Regarding the thickness influence on temperature, it can be noticed that the temperature decreases from one wall to another in all cases. This can be explained by the fact that the temperature decreases when the thickness of the receiver tubular decreases, being related to heat exchange through conduction. In reference to the materials performance analysis, the results presented in this paper proved that the most effective material is alloy 625, since it is fully austenitic and suitable for manufacturing. Moreover, it has excellent corrosion resistance in highly corrosive environments and is able to reach very high temperatures compared to other materials.

Nomenclature

Acronyms

3D: Three-Dimensional.

CFD: Computational Fluid Dynamics.

HTF: Heat transfer fluid.

$k-\varepsilon$: Turbulence model.

RB-STHX : Rod baffle shell-and-tube heat exchanger

Symbols

u_i: Instant fluctuation of x-velocity direction (m/s).
G_{kt}: Generation of turbulent kinetic energy due to the buoyancy force.
P_{kt}**:** Generation of the turbulent kinetic energy.
T: Fluctuation of temperature (K).
$\overline{T}$: The mean temperature (K).
$c_{3\varepsilon_t}$ and $c_{2\varepsilon_t}$: are coefficients
C_p: Specific heat (J/kg.K).
$\sigma_{\varepsilon t}$ and σ_{kt}: Turbulent Prandtl number.
ε : Kinetic energy Dissipation.
D: Height (cm).
ε_t : turbulent kinetic energy Dissipation.
i and j: ith and jth elements.
k_t: Turbulent kinetic energy.
L: Length (cm).
T: fluid Temperature (K)
u: Inlet velocity (m/s)
g: Gravity (m/s2)

k: Kinetic energy.
p: Pressure (Pa)
t: Total.
x: Coordinate system (i= x, y, z- j=x, y, z).
μ : Viscosity (kg/m s)
Nu: Nusselt number
Re: Reynolds number

R E F E R E N C E S

[1]. *D.-A. Ciupăgeanu, G. Lăzăroiu, and M. Tîrş*u, "Carbon dioxide emissions reduction by renewable energy employment in Romania," in 2017 11th International Conference on Electromechanical and Power Systems, SIELMEN 2017 - Proceedings, 2017, vol. 2017-Janua.

[2]. *P. R. Jayasree, A. Krishnan, A. S. Menon, M. Paul, and R. Rajin*, "Renewable energy integration," Int. J. Appl. Eng. Res., 2015.

[3]. *D.-A. Ciupăgeanu, G. Lazaroiu, and L. Barelli,* "Wind Energy Integration: Variability Analysis and Power System Impact Assessment," Energy, vol. 185, pp. 1183–1196, 2019.

[4]. *C. S. Power*, "Technology Roadmap Concentrating Solar Power," Current, 2010.

[5]. *M. S. Raboaca et al.*, "Concentrating solar power technologies," Energies. 2019.

[6]. *A. El-Leathy et al.*, "Thermal performance evaluation of two thermal energy storage tank design concepts for use with a solid particle receiver-based solar power tower," Energies, 2014.

[7]. *Y. Qiu, M. J. Li, W. Q. Wang, B. C. Du, and K. Wang*, "An experimental study on the heat transfer performance of a prototype molten-salt rod baffle heat exchanger for concentrated solar power," Energy, 2018.

[8]. *N. Boerema, G. Morrison, R. Taylor, and G. Rosengarten*, "High temperature solar thermal central-receiver billboard design," Sol. Energy, 2013.

[9]. *O. Garbrecht, F. Al-Sibai, R. Kneer, and K. Wieghardt*, "CFD-simulation of a new receiver design for a molten salt solar power tower," Sol. Energy, 2013.

[10]. *J. Samanes and J. Garcia-Barberena*, "A model for the transient performance simulation of solar cavity receivers," Sol. Energy, 2014.

[11]. *M. J. Montes, A. Rovira, J. M. Martínez-Val, and A. Ramos*, "Proposal of a fluid flow layout to improve the heat transfer in the active absorber surface of solar central cavity receivers," Appl. Therm. Eng., 2012.

[12]. *M. R. Rodríguez-Sánchez, A. Soria-Verdugo, J. A. Almendros-Ibáñez*, A. Acosta-Iborra, and D. Santana, "Thermal design guidelines of solar power towers," Appl. Therm. Eng., 2014.

[13]. *M. R. Rodríguez-Sánchez, C. Marugan-Cruz, A. Acosta-Iborra, and D. Santa*na, "Comparison of simplified heat transfer models and CFD simulations for molten salt external receiver," Appl. Therm. Eng., 2014.

[14]. *J. D. Osorio, R. Hovsapian, and J. C. Ordonez,* "Effect of multi-tank thermal energy storage, recuperator effectiveness, and solar receiver conductance on the performance of a concentrated solar supercritical CO 2 -based power plant operating under different seasonal conditions," Energy, 2016.

[15]. *X. Yang, X. Yang, J. Ding, Y. Shao, and H. Fan*, "Numerical simulation study on the heat transfer characteristics of the tube receiver of the solar thermal power tower," Appl. Energy, 2012.

[16]. *J. F. P. Pitot de la Beaujardiere, T. W. von Backström, and H. C. R. Reuter*, "Applicability of the local thermal equilibrium assumption in the performance modelling of CSP plant rock bed thermal energy storage systems," J. Energy Storage, 2018.
[17]. *M. S. Sohal, M. a Ebner, P. Sabharwall, and P. Sharpe*, "Engineering database of liquid salt thermophysical and thermochemical properties," Idaho Natl. Lab. Idaho Falls CrossRef, 2010.
[18]. *E. Oanta, C. Panait, M. L. Barhalescu, A. Sabau, and T. Axinte*, "Computer aided solution in an applied elasticity educational case study - Statically indeterminate system of bars," in 23rd DAAAM International Symposium on Intelligent Manufacturing and Automation 2012, 2012.
[19]. *N. Z. Ince and B. E. Launder*, "On the computation of buoyancy-driven turbulent flows in rectangular enclosures," Int. J. Heat Fluid Flow, 1989.
[20]. "ANSYS FLUENT 12.0 Theory Guide. ANSYS, Inc," 2009.